ELSEVIER

Journal of Organometallic Chemistry 491 (1995) 231-245

Journal of Organo metallic Chemistry

Lone-pair ligand effects on the oxidative addition of methane to second-row transition metal complexes

Per E.M. Siegbahn

Department of Physics, University of Stockholm, Box 6730, S-113 85 Stockholm, Sweden

Received 9 September 1994;

Abstract

The effects of lone-pair ligands on the oxidative addition of methane to metal complexes of the second transition series have been studied. The results are compared with those from similar previous studies for the naked transition metal atoms and for metal-hydrides and halides. The model complexes chosen for the present study are the M(CO), the MCl(CO) and the MH(CO) systems. The lowest energy at the SCF optimized transition state for the methane reaction for all these systems is found for RhCl(CO). This result is particularly interesting because the only second-row transition metal complexes that have been found to activate methane experimentally are Rh(I) complexes with halide (or Cp®) and lone-pair ligands. The main ligand effects involved are an attractive lone-pair ligand effect resulting from covalent sd_σ-hybridization and a cationic promotion effect. The presence of the halide makes the metal more cationic and the cations of the metals to the right have s^0 ground states, which have a low repulsion towards methane. The attractive lone-pair ligand effect is particularly well illustrated by the qualitatively different geometric ground states for the products of the reaction of methane with MCl(CO) and MH(CO) for the metals to the right. The methane reaction is also compared to the corresponding hydrogen molecule reaction.

Keywords: Yttrium; Zirconium; Niobium; Molybdenum; Technetium; Ruthenium

1. Introduction

During the past decade the detailed knowledge and the understanding of the bonding in small molecules containing transition metals has improved considerably and reached a high degree of sophistication. This understanding has been based on both accurate quantum chemical calculations [1] and on detailed experimental studies of cationic [2] and, more recently, of neutral gas phase systems [3,4]. When the results of these studies are analyzed, the spectral properties of the transition metal atoms are often emphasized. This spectroscopic aspect adds a new dimension to the more conventional chemical understanding of transition metal complexes. An interesting question in this context is to what extent the spectroscopic, valence-bond type, picture can be extended from small transition metal molecules, where it has been extremely useful, over to the larger realistic transition metal complexes actually used in catalytic processes.

In the present project an attempt has been made to bridge the gap between these two types of systems in a systematic way. This is done by studying key catalytic reactions such as oxidative addition [5], olefin insertion [6] and carbonyl insertion [7]. In the first step of the application of this approach to the case of the oxidative addition reaction, the reactions between methane and the bare metal atoms and cations were studied [8,9]. In the next step, the oxidation state of the metal was varied in a step-wise saturation of all the covalencies of the metal by adding hydrogen ligands [10]. In the third step, the hydride ligands were replaced by halide ligands to reveal the effects on the methane reaction of increasing the electronegativity of the ligands [11]. In the present paper, the effects of having lone-pair ligands on the C–H activation of methane is studied for complexes of the entire sequence of second-row transition metal atoms. The combined effects of hydride and lone-pair ligands, as well as halide and lone-pair ligands, are also studied. The largest complexes reached

SSDI 0022-328X(94)05238-7

at the end of this study are of the general form MXL, where X is a halide and L a lone-pair ligand. This type of system is still somewhat smaller than species actually observed to activate methane, for example $RhXL_2$ containing bulky ligands [12], but the main electronic structure aspects are believed to be present in the model systems. Steric effects are not considered at this stage, but can be studied later using molecular mechanics methods where structures of the present type can be used, as for example, has been done recently for the Ziegler-Natta reaction [13,14].

Only a few transition metals are represented among the metal complexes that have been observed to insert into C–H bonds in saturated hydrocarbons by an oxidative addition mechanism. The first observations of alkane C–H insertion in solution were made in 1982 for iridium complexes, where the active intermediates were believed to be coordinatively unsaturated fragments of the general formula Cp®IrL (L = CO,PR_3) [15,16]. Shortly afterwards the analogous rhodium fragment (Cp®RhL) was found to be active [17] and later the $ClRhL_2$ (L = PPh_3) fragment [12]. It is noteworthy in the present context that the small number of metals observed to be active implies that there are very special electronic structure requirements for oxidative addition. Furthermore, a strongly electronegative ligand such as Cl or Cp, and lone-pair ligands, such as CO or PPh_3, are present in all such cases.

The present study of lone-pair ligand effects is a natural continuation of three previous studies of the oxidative addition reaction for second-row transition metal complexes. In the first of these studies, the reactivity between the naked transition metal atoms and methane was studied [8]. By removing the ligands it was possible to isolate the factors of main importance for the metal itself in these reactions. Three main conclusions concerning the electronic structure aspects emerged from that study and from other similar previous theoretical studies of the oxidative addition reaction [18,19].

First, the main state involved in the binding in the insertion products for the methane reaction is the s^1-state (or longer, the $d^{n+1}s^1$-state). For the second row atoms to the left, there are also important contributions from s^1p^1-states (or longer, $d^ns^1p^1$-states). The second main conclusion is that in the transition state the s^0-state (or longer, the d^{n+2}-state) plays a key role. It is the presence of this low-lying state that leads to the lowest barriers for the atoms to the right, i.e. ruthenium, rhodium and palladium. In particular, the lowest barrier of the second row atoms is found for rhodium, because this atom has both low-lying s^0- and s^1-states. It is of interest in this context that rhodium complexes (see above) are the only second row complexes that have been found to activate alkanes [12,17,20]. The third main conclusion concerns the loss of exchange energy [8,21,22] in the reaction. This energy loss is particularly large for the atoms in the middle of the row, because there is a large number of unpaired 4d-electrons for these atoms. Therefore, the binding energies between naked metal atoms and practically any ligand will display a marked minimum in the middle of the row.

The second earlier study of the oxidative addition reaction, relevant in interpreting the results of the present study, was an investigation of covalent ligand effects [10]. Hydrogen atoms were chosen as covalent ligands, both because they are simple but also because the addition of hydrogen atoms lowers the spin of the complexes in a systematic way. The main results of that study are the following. First, promotion and exchange effects continue to play a dominant role for the effects of adding covalent ligands. If the promotion and exchange effects are subtracted from the results, two new trends can be identified. First, there is a systematic decrease in the reaction energies as one goes from left to right in the Periodic Table. This trend is attributed to the important role played by electron repulsion between the metal electrons and the ligand electrons, which increases with increasing number of metal electrons to the right in the row. The second trend is a systematic decrease of the reaction energies as the number of hydrogen ligands is increased. Because this effect is practically identical for the H_2 and the CH_4 reaction, the effect must be dominated by local rehybridization on the metal, which should be the same for hydrogen and methyl ligands, and not by steric effects. Two additional trends were noted in the previous study. First, the difference between the reaction energies for the H_2 and CH_4 reactions increases to the right of the Periodic Table. The second trend in the difference between the reaction energies of H_2 and CH_4 is more surprising. Even though methyl is bulkier than the hydrogen atom, the difference in reaction energy between H_2 and CH_4 decreases as the number of ligands increases. Both these trends are attributed to the fact that the repulsive effect between the metal and the ligands is also the dominant origin of the difference in the reaction energies between H_2 and CH_4. When more ligands are added, this repulsion is decreased both by local metal rehybridization and by electron transfer from the metal to the ligands.

In the third relevant earlier study of the mechanism of the oxidative addition reaction [11], the particular effects of halide ligands were best revealed by a direct comparison with the results for the corresponding complexes with hydride ligands. The main effects of replacing hydride by halide ligands for the oxidative addition reaction can simply be rationalized in terms of a more ionic bonding for the halides. For the complexes of the metals to the left, where the bonding is quite ionic for both the hydrides and the halides, interchanging these ligands will not have any major effects. For the atoms to the right, where the bonding is more covalent, the effects can be significant. For these systems there is a notable destabilizing effect of the halide ligands on the products of the reaction. The simplest way to understand this effect is to consider the metal as a cation when halide ligands are present. Since the bonding s^1 -state is higher in energy for the cations than for the neutral atoms to the right, the cations will form weaker bonds than the neutral atoms. In the transition state region, however, easy access to the s^0 state which is the ground state of the cations to the right, is an advantage. Because this state is the least repulsive state towards ligands, it allows the metal complex to approach close to methane for a more favourable interaction. The final size of the barrier is determined by a combination of how low is the repulsion in the entrance channel and how strong are the bonds in the product. Another consequence of the fact that the binding of the halides is more ionic than that of the hydrides is that the transition metal halides will have the same spin as the hydrides for the atoms to the left, but for the atoms to the right the halides will tend to have higher spin than the hydrides. In general this is an advantage for the halide complexes in cases where the high-spin state of the hydrides is high in energy. In the opposite situation, where the low-spin state is high in energy for the hydrides, it will be a disadvantage for the oxidative addition to replace the hydrides by halides.

2. Results and discussion

This section is divided into three subsections. In the first subsection the results for the reaction between methane and metal atoms with a single lone-pair ligand are discussed; the ligand chosen for this and also for the other studies in the present paper is carbonyl. In the second subsection a chloride ligand is also added to the metal to allow study of the combined effects of having halide and lone-pair ligands; a typical transition state structure for the methane reaction is shown in Fig. 1. In the third subsection the halide ligand is replaced by a hydride ligand; exchange of halide and hydride ligands was previously found to be an extremely useful procedure for isolating the particular effects of having more or less electronegative ligands on the metal. If a halide is simply added to a complex the effects of promotion and exchange loss energies will complicate the analysis, but if a hydride is replaced by a halide these effects will in most cases cancel in the comparison. In both the second and third subsection, the results for the methane reaction will be compared with those for the corresponding hydrogen molecule reaction.

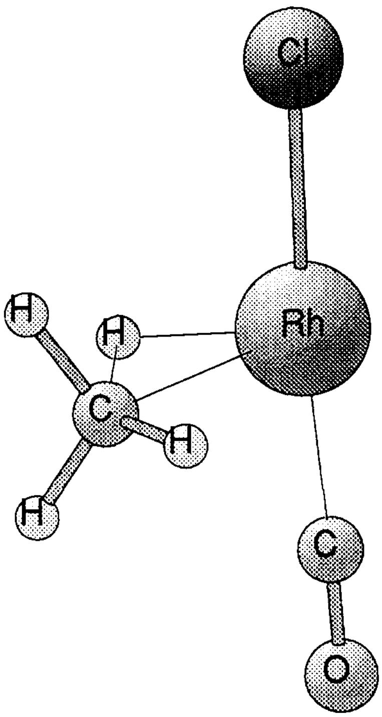

Fig. 1. The transition state for the reaction between RhCl(CO) and methane.

2.1. *The reactions between M(CO) and methane*

The results for the reactions between the second transition row M(CO) systems and methane are shown in Tables 1–4 and displayed in Figs. 2 and 3. The optimized geometries and binding energies of the products are listed in Table 1 with populations in Table 2. The energies are compared in Table 1 and in Fig. 2 with the corresponding data for systems without the carbonyl ligand. It should be noted that the results for the bare metal reactions are different from those published previously [8,10], because the new PCI-80 scheme has been used in the present study.

When the results for the M(CO) systems are compared with those for the ligand-free system, there are

Table 1
Geometries and energies for the oxidative addition reaction: MCO + $CH_4 + \Delta E \rightarrow M(CO)HCH_3$. The PCI-80 energies are calculated relative to ground state metal carbonyls and methane and include zero-point vibrational effects obtained for the rhodium systems. ΔE_0 is the corresponding result for the reaction between the bare metal and methane.

M	State	M–C_1	M–C_2	M–H	C_2–O	ΔE	ΔE_0
Y	^2A	2.37	2.37	2.04	1.17	−21.5	−20.9
Zr	^3A	2.25	2.28	1.92	1.16	−26.6	−20.5
Nb	^4A	2.29	2.37	1.85	1.14	−14.7	−17.3
Mo	^5A	2.21	2.43	1.77	1.13	−11.8	+3.2
Tc	^2A	2.11	1.92	1.67	1.15	−10.2	−1.8
Ru	^1A	2.07	1.91	1.59	1.14	−21.9	−9.7
Rh	^2A	2.07	2.13	1.56	1.13	−0.9	−18.8

Table 2
Populations for the products of the oxidative addition reaction: $MCO + CH_4 + \Delta E \rightarrow M(CO)HCH_3$.

Metal(M)	M(q)	4*d*	5*s*	5*p*	C_1(q)	C_2(q)	O(q)	H(q)
Y(^{2}A)	+.61	1.29	.47	.53	−.69	−.18	+.05	−.18
Zr(^{3}A)	+.43	2.39	.67	.44	−.67	−.10	+.10	−.17
Nb(^{4}A)	+.36	3.65	.56	.38	−.66	−.04	+.11	−.14
Mo(^{5}A)	+.29	4.74	.65	.27	−.65	−.00	+.12	−.10
Tc(^{2}A)	+.20	6.07	.45	.22	−.50	−.04	−.01	−.02
Ru(^{1}A)	+.08	7.28	.40	.18	−.44	−.02	+.01	+.02
Rh(^{2}A)	+.06	8.10	.48	.29	−.53	−.02	+.10	+.03

Table 4
Populations at the transition state of the oxidative addition reaction: $MCO + CH_4 + \Delta E \rightarrow M(CO)HCH_3$.

Metal(M)	M(q)	4*d*	5*s*	5*p*	C_1(q)	C_2(q)	O(q)	H(q)
Y(^{2}A)	+.08	1.54	.84	.45	−.53	−.09	+.04	+.06
Zr(^{3}A)	+.12	2.80	.71	.30	−.55	−.10	+.01	+.08
Nb(^{4}A)	+.09	4.10	.54	.21	−.52	−.08	+.04	+.06
Mo(^{5}A)	+.08	5.04	.56	.27	−.56	−.05	+.08	+.05
Tc(^{2}A)	+.07	6.31	.39	.16	−.48	−.06	−.04	+.11
Ru(^{1}A)	−.02	7.37	.43	.16	−.48	−.04	−.00	+.11
Rh(^{2}A)	+.03	8.18	.46	.27	−.56	−.04	+.08	+.07

two major effects. The first of these is quite general, and is one of the most important ligand effects found so far in the oxidative addition reaction of methane [23]. The effect is a result of covalent bonding and sd-hybridization, and therefore occurs preferentially to the right in the Periodic Table, where the bonding is more covalent than it is to the left. In Table 1 this effect is seen mainly for technetium and ruthenium. For these two atoms the spin is lowered when the carbonyl group is added to the $MH(CH_3)$ systems. The reason for this is that as the spin is lowered a hole is created perpendicularly to the C–M–H plane through sd_σ hybridization. This hole is perfectly suited for accepting the carbon lone-pair of the carbonyl and the metal therefore binds the carbonyl quite strongly. The sd_σ hybridization is also advantageous for the binding of the hydride and methyl products of the methane reaction, and methane and carbonyl therefore help each other to form a strongly bound product of the methane reaction. The gain in the methane reaction energy of adding the carbonyl lone-pair ligand is, according to the results in Table 1 and Fig. 2, 8.4 kcal mol^{-1} for technetium and as much as 12.2 kcal mol^{-1} for ruthenium. The reason for the larger gain for the ruthenium reaction is the presence of lower lying low-spin states for the ruthenium atom than for the technetium atom. There is an advantage of having low-lying low-spin states of the metal, because the gain in binding energy from the sd_σ hybridization effect has to be preceded by an initial promotion to a low-spin state of the metal.

Table 3
Geometries and energies for the transition state of the oxidative addition reaction: $MCO + CH_4 + \Delta E \rightarrow M(CO)HCH_3$. The PCI-80 energies are calculated relative to ground state metal carbonyls and methane, and include zero-point vibrational effects obtained for the rhodium systems. ΔE_0 is the corresponding result for the reaction between the bare metal and methane.

M	State	M–C_1	M–C_2	M–H	C_2–O	C_1–H	ΔE	ΔE_0
Y	^{2}A	2.47	2.34	1.98	1.16	1.56	+23.0	+20.7
Zr	^{3}A	2.38	2.17	1.87	1.16	1.55	+6.6	+16.9
Nb	^{4}A	2.29	2.12	1.80	1.15	1.52	+6.1	+15.6
Mo	^{5}A	2.26	2.17	1.77	1.14	1.54	+9.1	+37.8
Tc	^{2}A	2.21	1.91	1.65	1.16	1.50	+15.3	+23.8
Ru	^{1}A	2.20	1.90	1.60	1.15	1.51	+4.5	+10.9
Rh	^{2}A	2.15	2.05	1.69	1.14	1.58	+5.6	−1.4

As can be seen from Table 1 and Fig. 2, the reaction for rhodium is more exothermic without than with the carbonyl ligand, in contrast to the situation for ruthenium and technetium. The difference between these metals is easy to understand because rhodium has nine valence electrons and will therefore have all its *d*-orbitals occupied in the product complex. The rhodium atom will bind with its d^8s^1 state forming one *s*- and one *d*-bond to the hydride and the methyl group. The product cannot be lower than a doublet state, and one *d*-orbital therefore has to be singly occupied and will repel the carbonyl lone-pair. The reason why the reaction for rhodium is more endothermic with the car-

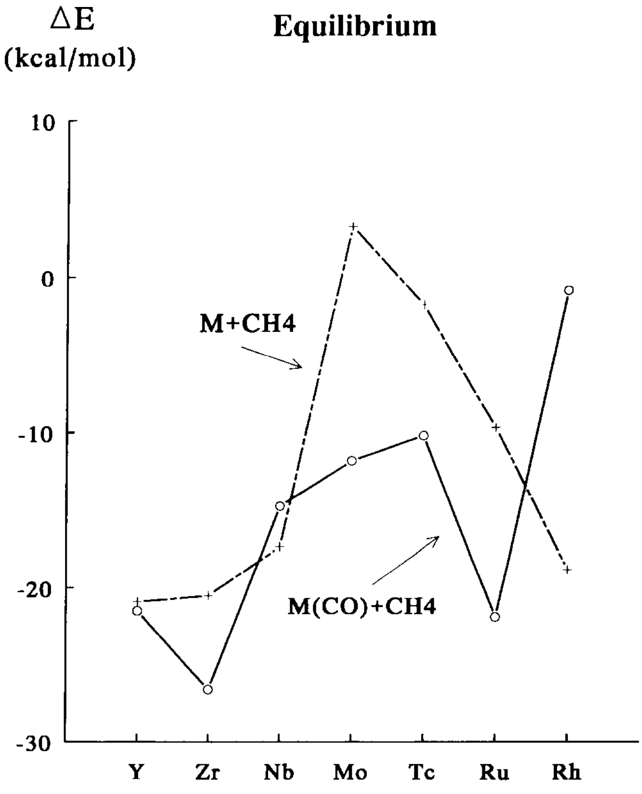

Fig. 2. The product energies for the reaction between the bare metal atoms M and methane, and for the reaction between M(CO) and methane.

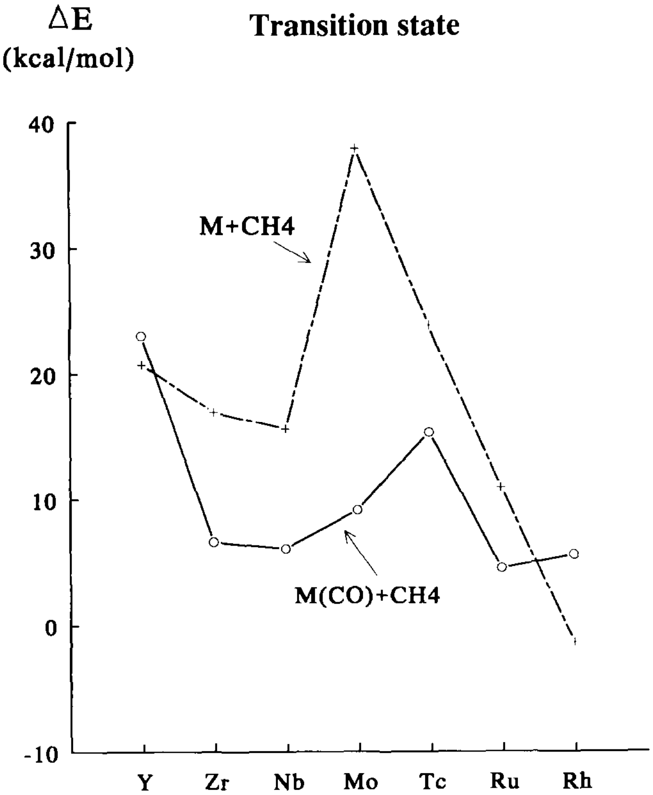

Fig. 3. The transition state energies for the reaction between the bare metal atoms M and methane, and for the reaction between M(CO) and methane.

bonyl ligand present is that in order to bind the hydride and methyl group, rhodium prefers to use its *s* -state, which is rather repulsive towards the carbonyl group. Before the reaction, rhodium can bind carbonyl with its less repulsive s^0 -state [7]. To remove the repulsion between the carbonyl ligand and the metal orbitals, it is important for rhodium to have still another, electron-withdrawing, ligand such as a halide as discussed below.

The second major effect evident from Table 1 and in Fig. 2 is best seen for zirconium. The product of the methane reaction for Zr(CO) is 6.1 kcal mol^{-1} more stable than that for the bare zirconium atom. The origin of this stabilization is a promotion effect. As already mentioned the most stable M–R bonds are formed when the metal uses its s^1-state. The zirconium atom has an s^2 ground state, and therefore needs to be promoted to form the bonds in the product of the methane reaction. In contrast, this promotion energy is already paid before the methane reaction for Zr(CO) which binds using the s^1-state [7]. For yttrium, which is the only other metal atom in the second transition series which has an s^2 ground state, there is no similar effect. This is because the yttrium atom also uses its s^2-state to form the bond in Y(CO). A promotion energy is therefore needed both for the bare yttrium atom and for Y(CO) when the bonds in the product of the methane reaction are formed, and the reaction energies will therefore be quite similar in the two cases. It should be added that the type of lone-pair ligand promotion effect noted for Zr(CO) cannot be expected to operate for more saturated systems because in those the s^1-state is likely to be dominant, whether or not lone-pair ligands are present.

The rather large stabilization of the methane reaction for molybdenum has a different origin from that of the other two effects described above. The molybdenum atom is a high-spin septet state, which has a very large exchange stabilization energy. This leads to a poor *sd*-hybridization for the molybdenum atom and the carbonyl ligand therefore hardly binds at all in Mo(CO), with an energy of only 1.7 kcal mol^{-1}. The Mo–C bond distance in Mo(CO) is very long at 3.9 Å. When the products of the methane reaction are bound to the molybdenum atom some sd-hybridization is introduced, which is apparently enough to form a much better bond to carbonyl. The carbonyl binding energy in $MoH(CH_3)(CO)$ is 15.2 kcal mol^{-1}, and there is a more normal Mo–C bond distance of 2.4 Å. It should be noted that this effect for molybdenum is not the same as the sd_σ hybridization effect discussed above for technetium and ruthenium. First, there is no lowering of the spin for the molybdenum complex as the carbonyl is bound. Secondly, a characteristic consequence of the sd_σ hybridization effect is that the carbonyl binds perpendicularly to the C–M–H plane. For molybdenum, the optimal position of the carbonyl ligand is in the C–M–H plane.

Most of the effects noted above for the products of the methane reaction are present also at the transition state, see Table 3 and Fig. 3. There is thus a lowering effect of carbonyl ligands on the barriers for the methane reaction for zirconium, molybdenum, technetium and ruthenium. However, the extents of the stabilizations are slightly different for the equilibrium geometries and the transition states. At the transition state, technetium is more stabilized than ruthenium. This effect is best understood by a comparison to molybdenum. Both technetium and molybdenum are very rigid as atoms owing to their high ground state spins, and this leads to very high barriers for the methane reaction for these atoms. As the spin is lowered, the hybridization flexibility is increased substantially, which is particularly important at the transition state. Ruthenium already has a higher hybridization flexibility as an atom, and the carbonyl ligand effect is therefore not as large as for the transition state of technetium.

For the atoms to the left, there is a lowering effect of having a carbonyl ligand on the barrier for zirconium but no effect for yttrium. Again, this is because of the promotion to the less repulsive s^1 state that occurs for Zr(CO) but not for Y(CO). Niobium, which has an

s^1 ground state, is somewhat different at the transition state than at the product equilibrium. In the transition state, the sd_σ hybridization effect is clearly seen, with the carbonyl coming in perpendicularly to the C–M–H plane and lowering the barrier. For rhodium finally, there is a much smaller destabilizing lone-pair ligand effect on the barrier than at the equilibrium geometry. The reason for this is that the s^0-state, which is the bonding state for Rh(CO), still dominates at the transition state in contrast to the case at the equilibrium where the s^1-state dominates.

The equilibrium and transition state geometries are quite similar to those discussed in detail previously for the bare metal reactions [8]. The d-populations are in all cases higher at the transition state than at the equilibrium geometries, which is a reflection of the fact that the repulsion is weaker for the d-electrons than for the s,p-electrons to methane. The size of the s,p-populations are less reliably given by the Mulliken population analysis because of the diffuse character of the orbitals, but it should be noted that these populations are actually somewhat higher at the transition state than at the equilibrium geometry for yttrium, in spite of the fact that these electrons are more repulsive towards methane. This is because of the s^2-character of the Y(CO) ground state. For the atoms to the left the total charges are much more positive at the equilibrium owing to the formation of the rather ionic M–R bonds. This effect is not seen for the atoms to the right because the bonds are much more covalent.

2.2. *The reactions between MCl(CO) and methane*

Before the reactions between MCl(CO) and methane are discussed, a few words should be said about the electronic and geometric structure of the isolated MCl(CO) systems. More details of these systems will be presented elsewhere. All the MCl(CO) systems are linear except those of yttrium and zirconium to the left. These optimal geometries can be understood in terms of an ionic $M^+Cl^-(CO)$ picture. The optimal electronic configuration of the M^+ cation is that which avoids repulsion towards Cl^- and the carbon lone-pair of CO. With sd-hybridization this leads to an optimal linear geometric configuration, because the metal charge is hybridized away perpendicular to the bonds in that case. This type of hybridization is dominant from niobium all the way to palladium to the right. For the atoms to the left, yttrium and zirconium, sp-polarization dominates instead, because these atoms have s^2 ground states. With sp-polarization, the charge is polarized away from Cl^- over to the back of the M–Cl bond. A linear approach of CO is therefore not optimal for these systems owing to the repulsion towards the carbon lone-pair. The bond angles in YCl(CO) and ZrCl(CO) are very similar, at 141.9° and 142.4° respectively. Most of the MCl(CO) systems have the same ground states as the corresponding MCl systems. The second-row transition metal chlorides have recently been described in detail and compared with the hydrides and fluorides [24]. The exceptions to the rule that the MCl(CO) and MCl systems have the same ground state occur for the systems to the left for yttrium and zirconium, which became non-linear as described above, and for ruthenium. For yttrium and zirconium, MCl(CO) also has higher spin than MCl. The reason for the increase in spin is that the low-spin configuration of YCl and ZrCl have s^2-occupations, which are too repulsive towards carbonyl. Another difference in ground state occupation is present in the case of ruthenium, where the RuCl(CO) has a $^4\Sigma^-$ ground state and RuCl a $^4\Pi$ ground state. Because the bonding to CO is stronger with doubly occupied π-orbitals, both of these orbitals become doubly occupied in RuCl(CO). For RuCl, repulsion towards Cl^- is smaller in the $^4\Pi$ state, which has one singly occupied π-orbital. The M–CO binding energies in the MCl(CO) systems are between 20 kcal mol^{-1} and 30 kcal mol^{-1} for all metals except yttrium, ruthenium and rhodium. For yttrium the promotion to a high spin state and the bending lead to a very small M–CO binding energy of only 6.7 kcal mol^{-1}. The M–CO bond in RuCl(CO) and RhCl(CO) are stronger than those for the other metals, at 43.9 kcal mol^{-1} and 36.0 kcal mol^{-1}, respectively. These metals can form the bonds required using their ground state d^ns^1 configuration. In contrast, a promotion to the s^1 state is needed for palladium.

The results for the products of the methane reaction with the MCl(CO) are shown in Tables 5 and 6 and the reaction energies are displayed in Fig. 4. For comparison the reaction energies for the corresponding H_2 reaction are also given in Table 5. The general nature of the differences between the M(CO) and MCl(CO) reactions is clearly displayed in Fig. 4. To the left, the addition of chlorine leads to a stabilization and to the right it leads to a destabilization. The dominant origin

Table 5
Geometries and energies for the oxidative addition reaction: $MCl(CO) + CH_4 + \Delta E \rightarrow MCl(CO)HCH_3$. The PCI-80 energies are calculated relative to ground state MCl(CO) systems and methane and include zero-point vibrational effects obtained for the rhodium systems. $\Delta E(H_2)$ is the result for the corresponding reaction with H_2.

M	State	M–C_1	M–C_2	M–Cl	M–H	C_2–O	ΔE	$\Delta E(H_2)$
Y	^1A	2.36	2.80	2.59	2.04	1.13	−26.9	−31.2
Zr	^2A	2.25	2.47	2.49	1.90	1.13	−29.3	−28.3
Nb	^3A	2.19	2.31	2.47	1.82	1.13	−24.8	−28.0
Mo	^4A	2.15	2.29	2.44	1.72	1.13	+2.3	−4.8
Tc	^3A	2.08	2.10	2.42	1.63	1.13	−1.0	−6.3
Ru	^2A	2.07	2.00	2.41	1.57	1.13	−8.5	−10.7
Rh	^1A	2.04	2.00	2.36	1.51	1.13	−21.6	−34.3

Table 6
Populations for the products of the oxidative addition reaction: $MCl(CO) + CH_4 + \Delta E \rightarrow MCl(CO)HCH_3$.

Metal(M)	M(q)	4*d*	5*s*	5*p*	C_1(q)	C_2(q)	O(q)	Cl(q)
Y(^{1}A)	+.69	1.14	.49	.54	−.68	+.01	+.16	−.42
Zr(^{2}A)	+.57	2.31	.51	.50	−.66	−.01	+.14	−.37
Nb(^{3}A)	+.49	3.48	.46	.50	−.61	+.01	+.13	−.38
Mo(^{4}A)	+.37	4.63	.52	.42	−.52	+.03	+.14	−.40
Tc(^{3}A)	+.30	5.71	.52	.41	−.46	−.02	+.10	−.42
Ru(^{2}A)	+.15	6.83	.52	.43	−.37	−.01	+.07	−.45
Rh(^{1}A)	+.01	8.01	.47	.44	−.33	+.03	+.10	−.42

of these trends are exchange loss effects, as described further below. An important exception to the general trends is found for rhodium, for which addition of a halogen atom leads to an increased stability. The calculated reaction energy for the RhCl(CO) reaction is -21.6 kcal mol^{-1}. This result for the rhodium system is particularly interesting because this system is quite similar to the only complexes of the second transition series found experimentally to activate methane, viz. Rh(I) complexes with halide (or Cp®) and lone-pair ligands [12,17]. The stabilization for the rhodium system because of the halide is easy to understand in terms of an ionic picture, because then chlorine simply transforms the electron configuration of rhodium in RhCl(CO) into that for ruthenium in Ru(CO), discussed above in the previous subsection. With this electron configuration rhodium can thus make one of its *d*-orbitals empty and leave space for the carbonyl lone-pair. The effect can also be understood with a more covalent picture of the bonding, because chlorine will then bind to the singly occupied *d*-electron in $RhHCH_3(CO)$ and move it partly out of the way from the carbonyl lone-pair. It should finally be noted that in line with the same electron count for Ru(CO) and RhCl(CO), for Ru(CO) the binding of the products of the methane reaction is very similar to that for RhCl(CO).

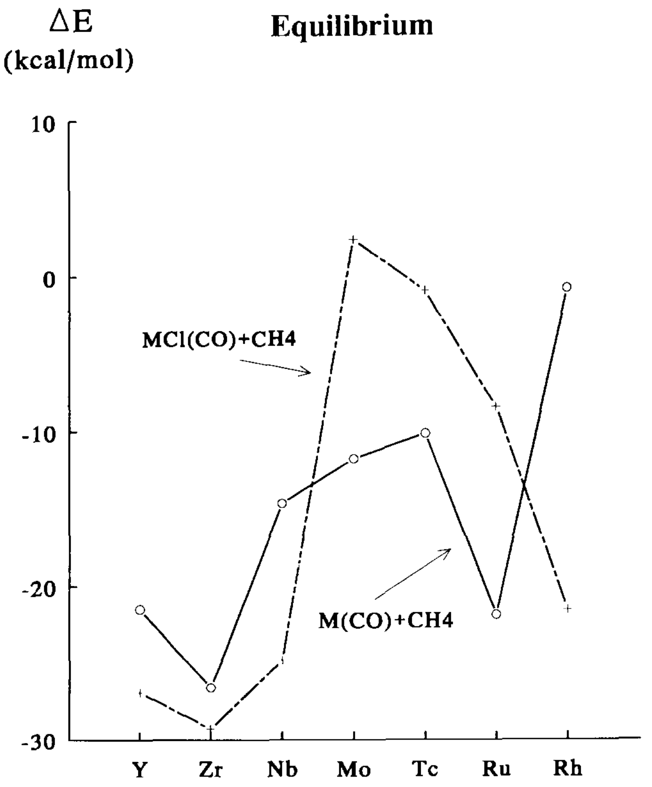

Fig. 4. The product energies for the reaction between MCl(CO) and methane, and for the reaction between M(CO) and methane.

With the large halide stabilization observed for the rhodium complex, it is perhaps surprising that the halide effect for the ruthenium complex is in exactly the opposite direction. For ruthenium the addition of the halogen atom changes the reaction energy from -21.9 kcal mol^{-1} to -8.5 kcal mol^{-1}, i.e. there is a large destabilization. There are mainly two reasons for this effect. The first is that there is a difference in the loss of exchange energy with and without the halide ligand. Upon adding a chlorine atom to Ru(CO) the spin state increases from a triplet to a quartet. This means that as the two bonds to hydrogen and methyl are formed there will be a rather large loss of exchange energy. This explanation based on exchange energy loss is further supported by the results for technetium, for which a relatively large destabilization is also found for the addition of the chlorine because the spin is increased. The second reason for the destabilization found upon adding chlorine in the methane reaction with Ru(CO) is that ruthenium in RuCl(CO) is more cationic than in Ru(CO). The origin of this effect is that for the neutral metal atoms to the right the bonding s^1-state is, in most cases, the ground state. For the cations, however, the ground state is normally the s^0 state. This means that to form the bonds in the product, the cation has to be promoted. There is thus a loss of promotion energy, leading to weaker bonds for the cations than for the neutral atoms. The bonds of the products for RuCl(CO) should be weaker than they are for Ru(CO) owing to this cationic promotion effect.

There is a reaction stabilization of 3–10 kcal mol^{-1} upon the addition of the chlorine atom for the atoms to the left. The origin of this stabilization is somewhat different for yttrium on the one hand, and zirconium and niobium on the other. The stabilization of the yttrium reaction is a result of a promotion effect. The yttrium atom has an s^2 occupation in Y(CO) but an s^1 occupation in YCl(CO). The s^1 occupation is better for binding the R-products of the methane reaction. This is exactly the same type of promotion effect as that discussed in the previous subsection for Zr(CO). The chlorine stabilization of the ZrCl(CO) and NbCl(CO) reactions are a result of changes in the exchange energy loss of exactly the same type, but of a different sign, as those for ruthenium and technetium discussed above. For both zirconium and niobium the spin is higher for M(CO) than for MCl(CO). The exchange stabilization is larger for niobium because this system has a higher spin. The stabilization for niobium is 10.1 kcal mol^{-1}, and that for zirconium 2.7 kcal mol^{-1}. It should be added that the cationic promotion effect which lowers the bond strengths to the right, as discussed above for RhCl(CO), is not present for the systems to the left. For these atoms neither the cations nor the neutral atoms have s^0 ground states as do the cations to the right.

The halide ligand effect for molybdenum requires a special explanation. The destabilization of 14.1 kcal mol^{-1} when chlorine is added cannot be explained in terms of exchange loss because the spin is actually lower for MoCl(CO) than for Mo(CO). In the previous subsection it was found that when the reaction for Mo(CO) is compared with that of the bare metal atom, there is a carbonyl stabilization effect of 15.0 kcal mol^{-1}. The origin of this effect is a large stabilization of the carbonyl binding energy because of the *sd*-hybridization induced by the bonding to the R-groups. The rigid molybdenum atom binds carbonyl very poorly. This type of stabilization effect does not occur for the MCl(CO) reaction because the carbonyl is already significantly bound before the reaction. The binding energy of the carbonyl to MoCl is 29.7 kcal mol^{-1} compared with only 1.7 kcal mol^{-1} for the molybdenum atom. Because this carbonyl stabilization effect is missing for the MoCl(CO) reaction, it seems as though the chlorine ligand has a destabilizing effect on the reaction.

A comparison of the methane reaction with the hydrogen molecule reaction, also shown in Table 5, reveals that the H_2 reaction is more exothermic (except for zirconium), as expected. The difference in reaction energies between these two reactions is not constant for the various metal atoms. With some slight deviations there is a trend towards increasing energy differences on going to the right in the Periodic Table. The reason for this trend is that the metal–methyl bonds tend to be weaker to the right owing to a larger repulsion to the increasing number of *d*-electrons. Because the hydrogen atom has fewer electrons than the methyl group, hydrogen is less sensitive to this type of repulsive effect. (This feature was noted and discussed in more detail in Ref. [10].) A notable exception to the increase in the energy difference between the H_2 and CH_4 reactions on going to the right is found between yttrium and zirconium. The reaction energy difference for yttrium is 4.3 kcal mol^{-1} but that for zirconium is actually negative by −1.0 kcal mol^{-1}. The origin of this effect is probably changes of hybridization; it is reasonable that the hybridization should affect the binding energy difference between methyl and hydrogen because this difference depends on the details of the repulsion towards the metal electrons. Before for yttrium, *sp*-polarization dominates and afterwards *sd*-polarization. For the atoms to the right, *sd*-polarization dominates both before and after the reaction. The reason *sp*-polarization is particularly important for yttrium is that this atom has the most stable s^2 ground state. As a final comment on the energy differences between the H_2 and CH_4 reactions, it can be noted that these differences are rather similar to those found in the absence of the carbonyl ligand [11]. The most important aspect of this result in the present context is that it constitutes a reliable check on the present calculations, and shows that there is complete consistency with the previous calculations. This is a far from trivial aspect of the present type of calculation. In fact, several errors were detected before this consistency was achieved.

Table 7

Geometries and energies for the transition state of the oxidative addition reaction: $MCl(CO)+CH_4+\Delta E \rightarrow MCl(CO)HCH_3$. The PCI-80 energies are calculated relative to ground state MCl(CO) systems and methane and include zero-point vibrational effects obtained for the rhodium systems.

M	State	M–C_1	M–C_2	M–Cl	M–H	C_2–O	C_1–H	ΔE
Y	^1A	2.48	2.33	2.59	1.97	1.16	1.55	+18.5
Zr	^2A	2.32	2.27	2.53	1.89	1.14	1.50	+5.3
Nb	^3A	2.47	2.21	2.47	1.74	1.14	1.62	+5.4
Mo	^4A	2.25	2.15	2.51	1.74	1.13	1.59	+21.5
Tc	^3A	2.20	2.10	2.44	1.62	1.13	1.63	+15.0
Ru	^2A	2.13	2.00	2.42	1.58	1.14	1.77	−2.2
Rh	^1A	2.14	2.00	2.37	1.54	1.13	1.71	−7.4

The most interesting result from a general consideration of the data in Table 7, is the low energy found for the SCF transition state structure for the rhodium system. The calculated energy is 7.4 kcal mol^{-1} below the reactant asymptote, and this is the lowest energy of all those in the table. This strongly supports the present type of modelling. It is argued that with a strongly electronegative ligand such as chlorine and a lone-pair ligand such as carbonyl, all the important electronic effects should be present for the RhCl(CO) system. In line with this assumption, this system behaves very much like the Rh(I) systems actually observed to acti-

Table 8

Populations at the transition state of the oxidative addition reaction: $MCl(CO)+CH_4+\Delta E \rightarrow MCl(CO)HCH_3$. H_2 is the hydrogen atom in the C–H bond that is being broken.

Metal(M)	M(q)	4*d*	5*s*	5*p*	C_1(q)	C_2(q)	O(q)	H_2(q)	Cl(q)
Y(^1A)	+.51	1.66	.30	.37	−.55	−.10	+.05	+.08	−.44
Zr(^2A)	+.39	2.68	.40	.43	−.53	−.04	+.08	+.04	−.41
Nb(^3A)	+.37	3.67	.51	.39	−.55	−.02	+.11	+.03	−.39
Mo(^4A)	+.35	4.77	.45	.38	−.52	+.02	+.11	+.04	−.46
Tc(^3A)	+.22	5.83	.49	.40	−.43	−.04	+.09	+.14	−.44
Ru(^2A)	+.15	6.89	.47	.41	−.38	−.03	+.07	+.15	−.45
Rh(^1A)	+.02	8.05	.45	.42	−.39	+.02	+.09	+.16	−.41

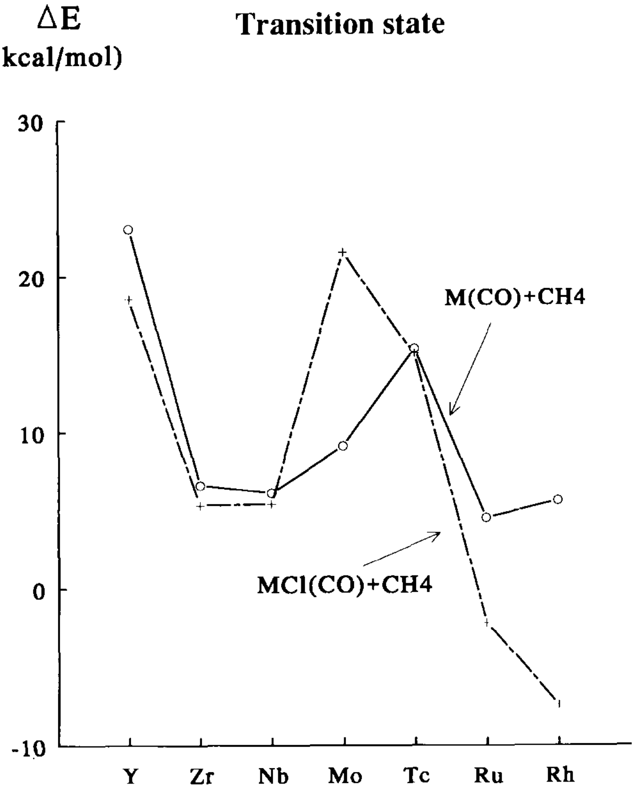

Fig. 5. The transition state energies for the reaction between MCl(CO) and methane, and for the reaction between M(CO) and methane.

vate the C–H bond in methane [7,12]. As a technical comment it can be added that even though the SCF transition state does not reveal a barrier at the higher level of calculation, the geometry is still characteristic C–H bond breaking with, for example, a long C–H for the bond distance. The energy at this point is therefore still relevant for the discussion of the ability to break the C–H bond.

Another interesting result in Table 7, also clearly seen in Fig. 5, is that the C–H activation barriers for most of the MCl(CO) systems are lower than for both the M(CO) systems and the bare metal atoms. The only exception is found for molybdenum in the middle of the row. For the atoms to the left the main reason for the lower barriers for the MCl(CO) systems is a smaller loss of exchange energy. For the atoms to the right there are two main reasons for the lower barrier. The first is that the metals in MCl(CO) are more cationic than they are in M(CO) and in the bare metal atoms. Because the cations to the right have s^0 ground states the access to this state is easier for the MCl(CO) than it is for M(CO) or M. It has been pointed out that for the bare neutral atoms [8] and for the cations [9], the access to the s^0 state, which is the least repulsive state, is very important for a low barrier for the methane reaction. Easy access to the s^0 state is thus the main reason why the barriers for C–H and C–C activation are lower to the right for the bare metal atoms. The other main reason for the low barrier of the MCl(CO) systems is the attractive lone-pair ligand effect. For the MCl(CO) systems both the halide and the carbonyl feel the attraction created by the *sd*-hybridization.

It is interesting to compare the barrier heights and reaction energies for Ru(CO) and RuCl(CO) because this illustrates an important balance of effects present in the C–H activation reaction. The reaction energy is -21.9 kcal mol^{-1} for Ru(CO) and -8.5 kcal mol^{-1} for RuCl(CO); i.e. the product of the reaction with Ru(CO) is much more stable. Yet, the transition state energy for the reaction is substantially lower for RuCl(CO), viz. -2.2 kcal mol^{-1} compared with $+4.5$ kcal mol^{-1} for Ru(CO). These apparently conflicting differences in product energies and barrier heights can be rationalized in terms of differences in the exchange energy loss and the cationic promotion effects. At the equilibrium geometry the cationic promotion effect and the exchange energy loss effect work in the same direction, but at the transition state they have opposite signs. The exchange energy loss effect leads to weaker bonds and higher transition states for RuCl(CO) because it has a higher spin than Ru(CO). This effect should be larger at the equilibrium geometry where the bonds are fully formed. The cationic promotion effect leads to weaker bonds at the equilibrium but to lower

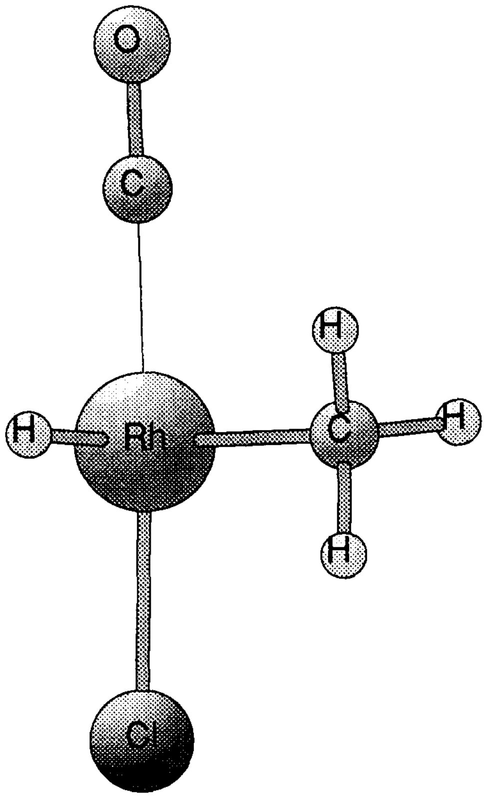

Fig. 6. The equilibrium geometry for the product of the reaction between RhCl(CO) and methane.

transition states for RuCl(CO). At the transition state the cationic promotion effect appears to be somewhat more important, because the barrier is lower for RuCl(CO) than it is for Ru(CO). An additional effect may also be of some importance for the difference in barrier heights, namely that for RuCl(CO) two ligands feel the attraction because of the *sd*-hybridization effect while for Ru(CO) only one ligand is affected.

The equilibrium geometry of the product for the reaction between RhCl(CO) and methane, shown in Fig. 6, illustrates the main lone-pair ligand effect of this reaction. Methane approaches rhodium in one plane, and perpendicular to this plane the *sd*-hybridization effect, induced by the formation of the covalent M–R bonds, creates holes in the electron density. The chloride and the lone-pair of the carbonyl occupies this space. The attractive effect is illustrated by the changes in the bond distances. The rhodium–carbonyl (Rh–C) bond distance decreases from 2.12 Å in RhCl(CO) to 2.00 Å at both the transition state and the equilibrium product geometry of the methane reaction. The changes in the rhodium–chloride bond distance are somewhat smaller, at 2.43 Å for RhCl(CO) and at 2.37 Å and 2.36 Å at the transition state and equilibrium respectively.

2.3. *The reactions between MH(CO) and methane*

Some of the effects from adding chlorine to the M(CO) systems were identified above as promotion and exchange energy loss effects. These types of effects should also be approximately the same if hydrogen is added to the M(CO) systems. In order to identify the specific effects of a more or less electronegative ligand or the effects resulting from donation from the halide lone-pairs, it is therefore useful to compare the results for the methane reaction for MCl(CO) with those for MH(CO). The MH(CO) were considered in detail in Ref. [7] in connection with the carbonyl insertion reaction. Because the ground states for the MH and MCl systems are the same for most metals [24], and the ground state for MX(CO) is the same as for MX for most metals, the ground states for MH(CO) and MCl(CO) are also the same for most metals. The main exceptions are found to the right for ruthenium and rhodium. In contrast to the MCl(CO) systems, the MH(CO) systems for these metals prefer bent structures and low spin ground states, and this has consequences for the methane reaction, as will be shown below. To the left, the MH(CO) systems are quite similar to the MCl(CO) systems, which is in line with what is generally found. For the metals to the left, where ionicity in the bonding dominates owing to the low ionization potentials of the metals, it is normally qualitatively adequate to use the simpler hydride ligands as models for halide ligands.

Table 9

Geometries and energies for the oxidative addition reaction: $MH(CO)+CH_4+\Delta E \rightarrow MH(CO)HCH_3$. The PCI-80 energies are calculated relative to ground state MH(CO) systems and methane and include zero-point vibrational effects obtained for the rhodium systems. $\Delta E(H_2)$ is the result for the corresponding reaction with H_2.

M	State	$M-C_1$	$M-C_2$	M–H	C_2-O	ΔE	$\Delta E(H_2)$
Y	^1A	2.38	2.83	2.06	1.13	−25.9	−29.9
Zr	^2A	2.26	2.46	1.93	1.13	−29.4	−26.8
Nb	^3A	2.20	2.30	1.84	1.13	−20.6	−21.9
Mo	^4A	2.16	2.45	1.74	1.13	+0.6	−2.0
Tc	^3A	2.13	2.22	1.65	1.13	+2.3	−4.0
Ru	^2A	2.08	2.18	1.59	1.13	+8.4	+2.6
Rh	^1A	2.04	2.13	1.52	1.13	−3.3	−13.2

The results for the MCl(CO) reactions are compared with those for MH(CO) in Tables 9 and 10 and in Fig. 7, the main features are as follows. First, all the results for the systems of the metals to the left are very similar; as mentioned several times, this is a quite general feature. Secondly, the results for the metals in the middle of the row, molybdenum and technetium, are also quite similar. This is probably the best illustration of the usefulness of the present approach in which the effects of hydride and halide ligands are compared for otherwise identical systems. As shown in the previous subsection, the effects of *adding* a chlorine atom to a complex is often very large in the middle of the row, where the exchange loss effects are normally largest because the spin is highest for these systems. It is therefore difficult to separate out the particular effects of halide ligands from these exchange effects if a halogen atom is just added to a complex. The final feature, revealed by comparing Tables 5 and 9 is that the results for ruthenium and rhodium are quite different.

There are two important reasons for the fact that the results for the MH(CO) systems are different from those for the MCl(CO) systems for ruthenium and rhodium. The first is that for these metals the reactants have different ground states. The ground state for RhH(CO) is a bent singlet and the adiabatic excitation energy to the linear triplet state, which is the ground state for RhCl(CO), is 22.6 kcal mol^{-1}. This promotion

Table 10

Populations for the products of the oxidative addition reaction: $MH(CO)+CH_4+\Delta E \rightarrow MH(CO)HCH_3$.

Metal(M)	M(q)	4*d*	5*s*	5*p*	C_1(q)	C_2(q)	O(q)	H(q)
Y(^{1}A)	+.55	1.11	.58	.66	−.70	−.00	+.16	−.20
Zr(^{2}A)	+.46	2.28	.60	.57	−.67	−.03	+.13	−.17
Nb(^{3}A)	+.37	3.52	.52	.53	−.64	−.01	+.12	−.13
Mo(^{4}A)	+.29	4.67	.63	.36	−.62	+.02	+.12	−.09
Tc(^{3}A)	+.23	5.79	.59	.34	−.60	−.01	+.09	−.04
Ru(^{2}A)	+.10	6.98	.54	.31	−.55	−.00	+.09	+.00
Rh(^{1}A)	−.10	8.20	.48	.36	−.51	−.00	+.09	+.07

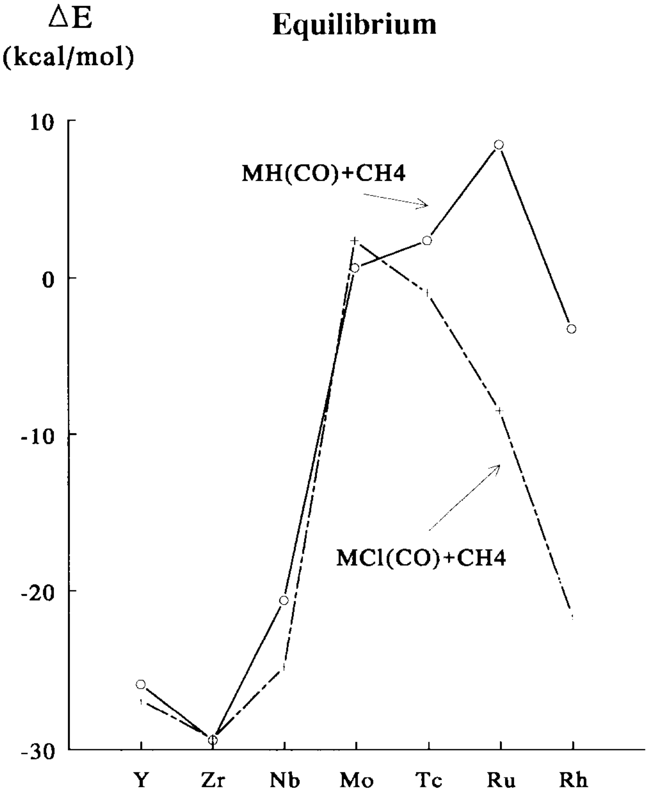

Fig. 7. The product energies for the reaction between MH(CO) and methane, and for the reaction between MCl(CO) and methane.

energy should thus in principle be paid to form the M–R bonds in the product. This is by far the most important factor because the difference between the methane reaction energies for Rh(CO) and RhCl(CO) of 18.3 kcal mol^{-1} is quite similar to the promotion energy. The second part of the explanation for the differences between the reaction energies of RhH(CO) and RhCl(CO) can be seen from Fig. 8. When the equilibrium geometry of the product of the methane reaction for RhH(CO) is compared to that for RhCl(CO) in Fig. 6, it can be seen that they are qualitatively different. This difference is one of the most interesting results from the present study. As described in the previous subsection, the important lone-pair ligand effect on the methane reaction is found to the right, owing to the *sd*-hybridization induced by the formation of the covalent M–R bonds. For the RhCl(CO) reaction this effect creates holes in the electron cloud perpendicular to the R_1–M–R_2 plane and these holes can be used by the carbonyl lone-pair and the halide ligands to strengthen the bonding to the metal. During the reaction the M–Cl and M–CO bonds are gradually strengthened, and this lowers the barrier and increases the exothermicity. For the RhH(CO) reaction this same type of effect has a quite different consequence on the geometry. For the product of this reaction there are not two but *three* strongly covalent bonds. In contrast to the situation for the MCl(CO) reaction, in which the two strongest covalent bonds of the product are the M–H and M–CH_3 bonds, the two strongest covalent bonds in the product of the MH(CO) reaction are the two M–H bonds. In both cases the lone-pair ligands want to orient themselves perpendicular to the plane formed by the two strongest covalent bonds. These directions are thus different for the two systems, as is nicely illustrated in Fig. 6 and Fig. 8. It should be added that the geometry of the transition state for the MH(CO) reaction is qualitatively the same as that for the product equilibrium in Fig. 8. When the fact that the lone-pair ligand effect is different for MH(CO) and MCl(CO) is appreciated, it is also easy to understand why the difference in the reaction energies of 18.3 kcal mol^{-1} is somewhat smaller than the promotion energy of 22.6 kcal mol^{-1} required to form the bonds for RhH(CO). The reason is that the lone-pair ligand effect is more important for RhH(CO) because the two M–H bonds in the product of this reaction are more strongly covalent than the one M–H and the one M–C bond formed in the product of the MCl(CO) reaction. The energy gain owing to the increased bonding of the lone-pair ligand is therefore somewhat larger for RhH(CO).

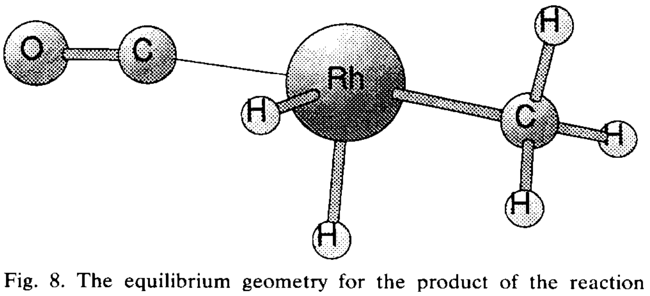

Fig. 8. The equilibrium geometry for the product of the reaction between RhH(CO) and methane.

The results for ruthenium are quite parallel to those for rhodium discussed above. RuH(CO) has a bent doublet ground state and has an adiabatic excitation energy to reach the linear quartet state of 14.5 kcal mol^{-1}. The transition state and the product of the RuH(CO) reaction have the carbonyl lone-pair ligand pointing perpendicular to the plane formed by the two Ru–H bonds. The reaction energy difference between the RuCl(CO) and RuH(CO) reactions is 16.9 kcal mol^{-1} in favour of the RuCl(CO) reaction. However, it can be noted that the difference between the adiabatic promotion energy difference 14.5 kcal mol^{-1} and the reaction energy difference of 16.9 kcal mol^{-1} is smaller and different in sign than for rhodium, for which the corresponding values are 22.6 kcal mol^{-1} and 18.3 kcal mol^{-1}. The most likely explanation for this difference between ruthenium and rhodium is that differences between the exchange energy loss effects are also involved because these are important for ruthenium but essentially absent for rhodium, as noted in the previous subsection. The exchange energy loss could, for example, be slightly different for the reaction energy and the adiabatic excitation energy. The extent to which there is *sd*-hybridization before the reaction could also have some effect. To separate out these effects, more results of the same type will be needed.

It is noteworthy that although the geometry shown in Fig. 8 for $RhH_2CH_3(CO)$ is the optimal geometry, the optimal geometry for $RhClHCH_3(CO)$ in Fig. 6 is a local minimum for $RhH_2CH_3(CO)$. The energy difference obtained between the optimal and the local minimum gives some idea of the magnitude of the sd_σ hybridization effect, which must be larger than the energy difference because the effect is present for both geometries. This energy difference is for rhodium 5.1 kcal mol^{-1}, for ruthenium 8.8 kcal mol^{-1} and for technetium 3.0 kcal mol^{-1}. For the $MH_2CH_3(CO)$ systems to the left of technetium there is only one minimum.

As in the case of the MCl(CO) reactions, the results for the reactions between the MH(CO) systems and H_2 provide an excellent check on those for the methane reaction. The MCPF reaction energy differences between the methane and the H_2 reactions for the MH(CO) systems are in all cases within 2 kcal mol^{-1} of the corresponding differences reported previously for the MH systems without the carbonyl ligand [10]. This close similarity is quite remarkable, because the carbonyl is of significant importance for the reaction through the lone-pair ligand effect. This similarity does not mean that the energy difference between the methane and H_2 reactions is the same for all metals. It varies between −2.6 kcal mol^{-1} for zirconium to the left and +9.9 kcal mol^{-1} for rhodium to the right. Again, the origin of this trend is the increased repulsion between the methyl group and the *d*-electrons on going to the right.

Few additional comments are needed concerning the results for the transition states of the methane reaction for MH(CO) shown in Tables 11 and 12 and in Fig. 9. The similarity between the MH(CO) results and the MCl(CO) results to the left is again striking, with the possible exception for niobium for which the lone-pair ligand effect appears to be more important for the MCl(CO) system. Niobium, with its s^1 ground state and *sd*-hybridization, shows some similarity to the systems to the right, where the barrier heights are always lower for the MCl(CO) systems. There are two causes of the lower barriers for the MCl(CO) systems to the right. First, there is the cationic promotion effect described above; because the chloride makes the metal more cationic the access to the s^0-state becomes easier because this is the ground state for the cations to the right. The s^0-state is important in the transition state

Table 11
Geometries and energies for the transition state of the oxidative addition reaction: $MH(CO)+CH_4+\Delta E \rightarrow MH(CO)HCH_3$. The PCI-80 energies are calculated relative to ground state MH(CO) systems and methane and include zero-point vibrational effects obtained for the rhodium systems. H_1 is the hydrogen atom in the reacting MH(CO) system.

M	State	M–C$_1$	M–C$_2$	M–H$_1$	M–H$_2$	C$_2$–O	C$_1$–H$_2$	ΔE
Y	^{1}A	2.49	2.33	2.06	1.98	1.16	1.55	+18.4
Zr	^{2}A	2.29	2.26	1.95	1.90	1.14	1.50	+2.9
Nb	^{3}A	2.35	2.15	1.92	1.84	1.15	1.54	+12.9
Mo	^{4}A	2.29	2.18	1.85	1.73	1.14	1.73	+20.2
Tc	^{3}A	2.20	2.18	1.75	1.63	1.14	1.59	+16.9
Ru	^{2}A	2.26	2.00	1.72	1.70	1.14	1.61	+14.2
Rh	^{1}A	2.12	2.05	1.53	1.54	1.14	1.70	+3.2

Table 12
Populations at the transition state of the oxidative addition reaction: $MH(CO)+CH_4+\Delta E \rightarrow MH(CO)HCH_3$. H_2 is the hydrogen atom in the C–H bond that is being broken.

Metal(M)	M(q)	4*d*	5*s*	5*p*	C$_1$(q)	C$_2$(q)	O(q)	H$_2$(q)
Y(^{1}A)	+.32	1.64	.45	.46	−.56	−.12	+.03	+.07
Zr(^{2}A)	+.17	2.71	.57	.47	−.53	−.04	+.06	+.03
Nb(^{3}A)	+.19	3.66	.64	.45	−.58	−.02	+.07	+.05
Mo(^{4}A)	+.14	4.73	.61	.46	−.46	−.05	+.09	+.03
Tc(^{3}A)	+.09	5.95	.52	.43	−.45	−.06	+.08	+.10
Ru(^{2}A)	+.06	7.27	.37	.24	−.55	−.05	+.03	+.10
Rh(^{1}A)	−.12	8.27	.48	.32	−.53	−.02	+.08	+.09

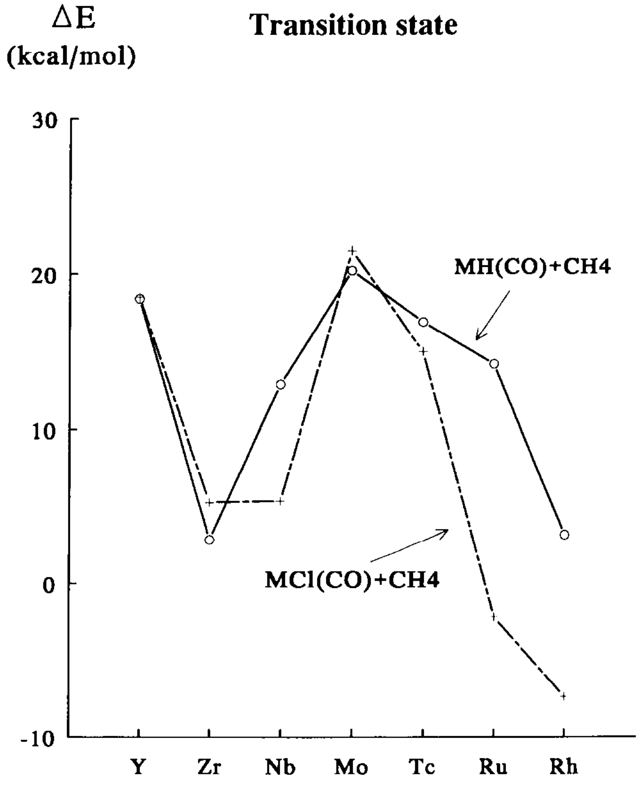

Fig. 9. The transition state energies for the reaction between MH(CO) and methane, and for the reaction between MCl(CO) and methane.

region because it has a low repulsion towards methane. The second cause of the lower barrier for the MCl(CO) systems to the right is that the MH(CO) systems have low-spin ground states for ruthenium and rhodium, and a promotion is therefore needed to form the bonds.

3. Conclusions

Oxidative addition of methane and that of the hydrogen molecule have been examined for a large number of second-row transition metal systems. The characteristic feature of the selected model systems is that they all have a carbonyl lone-pair ligand. Several important general effects in the oxidative addition reaction have been identified by comparison of the results with those of previous studies in which the methane reaction was investigated for the bare metal atoms, the metal cations, the metal-hydrides and the metal-halides. For the metals to the right the carbonyl ligand has a stabilizing effect on the reaction. This effect is because of an sd_σ hybridization induced by the formation of the M–R bonds. When the *sd*-hybrids are formed to optimize the bond strength of the M–R bonds, another *sd*-hybrid will automatically be formed perpendicular to the R–M–R plane. If this second *sd*-hybrid is empty there will be an attractive hole in the electron cloud which can be used by the carbonyl ligand to approach the metal more closely and form a stronger bond. The extent of *sd*-hybridization depends on the covalency of the bonding and so the effect is not seen for the metals to the left where the bonding is more ionic. An interesting demonstration of the *sd*-hybridization effect is found when the reactions of the MCl(CO) and MH(CO) systems are compared for the metals to the right. For the MCl(CO) system the carbonyl is oriented perpendicular to the H–M–CH_3 plane. In contrast, for the MH(CO) system, where the strongest covalent bonds of the product are the two M–H bonds, the carbonyl is oriented perpendicular to the H–M–H plane. The carbonyl also has a stabilizing effect for the methane reaction for most M(CO) systems to the left, but the origin of this effect is different and less general than it is for those to the right. For the atoms to the left, the carbonyl in M(CO) will promote the s^1 state, which is more favourable for forming the M–R bonds. Without the carbonyl, the ground state of the metal atoms to the left have s^2 ground states.

When the MH(CO) reactions are compared with those for the MCl(CO) reactions, the effects of having a more electronegative ligand that can donate electrons can be observed directly. For the atoms to the left, the results for the methane reaction are very similar for these two systems. However, for those to the right there are significant differences. These differences can be attributed to a cationic promotion effect. The neutral metal atoms to the right have s^1 ground states, but the metal cations have s^0 ground states that are ideally suited for approaching methane with a low repulsion. The MCl(CO) systems, where the metal is quite cationic, will therefore in general have lower barriers than the MH(CO) systems, where the metal is more neutral. In contrast, for the formation of the bonds in the products the s^1 state is more favourable. This advantage for the MH(CO) systems to the right is, however, more than counterbalanced by the fact that they have low spin ground states. Thus, both RuH(CO) and RhH(CO) have to be promoted to high spin states, which ultimately leads to more weakly bound products than for the reactions of the MCl(CO) systems, for which this type of promotion is not needed.

The results of the present study allow incorporation of the main electronic structural effects into the gradual and systematic development of model transition metal complexes. In line with this strategy, the results for the RhCl(CO) model system are quite similar to those found for actual rhodium complexes found experimentally to cause dissociation of methane such as $RhCl(PPh_3)_2$ or RhCp*(CO). The exothermicity for the methane reaction with RhCl(CO) is predicted to be 22 kcal mol^{-1} and the barrier for C–H activation essentially zero. One major effect not covered by the present approach is the effect of bulky ligands. This type of effect is, however, usually much easier to predict, and is therefore normally handled by the simpler molecular mechanics approach.

4. Computational details

In the calculations reported in the present paper of lone-pair ligand effects on the oxidative addition reaction of methane to complexes of second-row transition metal atoms, reasonably large basis sets were used in a generalized contraction scheme. All valence electrons, except the chlorine 3*s* electrons, were correlated using size consistent methods. The basis sets and underlying methods are identical to those used in the previous studies of the same type [5–11]. In short, the geometry optimizations are performed at the SCF level using the GAMESS set of programs [25] using double zeta quality basis sets. Computed Hessians were always used to locate the transition states, and were also determined whenever this was felt motivated. The accuracy of the geometry optimization step has recently been systematically tested and found to be adequate both for equilibrium and transition state geometries for cases where no coefficient in the configuration expansion of the preceding correlation calculation is larger than 0.20 [26]. The correlated calculations are performed using the Modified Coupled Pair Functional (MCPF) method

[27], which is a size-consistent, single reference state method. The zero-order wave-functions are in these cases determined at the SCF level. The basis sets in these calculations are larger than those used in the geometry optimization, with polarization functions on all atoms including an f-set on the metal. Because rotation between valence and core orbitals sometimes occurs, a localization of the core orbitals has to be performed, and this was done using a localization procedure in which $\langle r^2 \rangle$ of the core orbitals is minimized. Relativistic effects were accounted for using first-order perturbation theory including the mass-velocity and Darwin terms [28]. All these calculations were performed on an FX-80 ALLIANT and on an IBM Risc 6000 computer, and the final energy evaluations were performed using the STOCKHOLM set of programs [29].

Even though the absolute accuracy of the MCPF calculations is not very high, the fact that the errors are highly systematic can be used to significantly reduce the relative errors. The accuracy is mainly limited by the basis set size, but the lack of triples is another rather important factor. In comparison to these other errors, the error in the geometry optimization step can normally be neglected. Based on comparisons to calculations of high accuracy and on comparisons to experiments, it can be concluded that the present type of treatment gives about 80% of the valence correlation effects. A simple estimate of the remaining correlation effects is then obtained by simply adding 20% correlation energy to each system. This is the general idea behind the PCI-80 (Parametrized Configuration Interaction with parameter 80) scheme which has recently been proposed [30]. It was shown in Ref. [30] that this parametrization gives a major improvement of the results compared to an unparametrized treatment. For a benchmark test consisting of the atomization energies of 32 neutral first-row systems, the PCI-80 scheme gives an average absolute deviation compared to experiments of only 2.3 kcal mol^{-1}. Johnson et al. [31] have shown that for the same systems the MP2 method gives an average absolute deviation of 22 kcal mol^{-1} using polarized basis sets. This means that the PCI-80 scheme should be a significant improvement compared to the MP2 method, which has until now with a few exceptions been the highest level of treatment used for the present size of transition metal complexes. For transition metal systems the improvement at the PCI-80 level compared to an unparametrized treatment is sometimes quite dramatic. Tests against essentially all experimentally studied small second-row transition metal complexes show that the accuracy of the PCI-80 scheme for bond strengths is probably at least as high as that available from experiments for these systems [30]. For several first-row systems it was shown in Ref. [30] that a Hartree-Fock limit correction is also needed. This correction is usually small for transition metal systems. In fact, a useful approximation is to assume that these effects roughly cancel basis set superposition errors and $4s,4p$ correlation effects. This approximation has been used in the present study. In order to be directly comparable to experiments, the calculated energies have to be corrected for zero-point vibrational effects. These energies were calculated for all rhodium systems using the GRADSCF program [32] on a CRAY-YMP computer. The zero-point energies from the rhodium systems were used for all the other metals.

Finally, all the results reported here are for the ground state of each system. It should be noted that because, in most cases, the ground state of the reactants has a different total spin than the ground state of the products, this means that for a particular reaction the energies are given for different spin-states in the beginning and at the end of the reaction. This procedure is partly motivated by the ease to define conveniently what has been done. It is also motivated, however, by what actually happens in these reactions involving the relatively heavy second-row transition metal atoms. It has been shown in detail by Mitchell [3], that in the case of the association reaction between the nickel atom and carbon monoxide, the crossing probability between different spin surfaces is near unity because of the large spin-orbit coupling. Also, in order to rationalize the experimental results for the oxidative addition reaction between the nickel atom and water, a high crossing probability has to be assumed [33]. The crossing probability should be even larger for the present second-row transition metal systems.

References

[1] C.W. Bauschlicher, Jr. and S.R. Langhoff, in A. Dedieu (ed.), *Transition Metal Hydrides*, Ch. 3, VCH Publishers, NY, 1992.

[2] P.B. Armentrout, in J.A. Davies, P.L. Watson, A. Greenberg and J.F. Liebman (eds.), *Selective Hydrocarbon Activation: Principles and Progress*, VCH Publishers, NY, 1990 pp. 467–533.

[3] S.A. Mitchell, in A. Fontijn (ed.), *Gas-Phase Metal Reactions*, Ch. 12, Elsevier, Amsterdam, 1992.

[4] J.C. Weisshaar, in A. Fontijn (ed.), *Gas-Phase Metal Reactions*, Ch. 13, Elsevier, Amsterdam, 1992.

[5] P.E.M. Siegbahn and M.R.A. Blomberg, in P.W.N.M. van Leeuwen, J.H. van Lenthe and K. Morokuma (eds.), *Theoretical Aspects of Homogeneous Catalysis, Applications of Ab Initio Molecular Orbital Theory*, Kluwer Academic Publishers, 1994.

[6] (a) P.E.M. Siegbahn, *J. Am. Chem. Soc.*, *115* (1993) 5803; (b) P.E.M. Siegbahn, *Chem. Phys. Lett.*, *205* (1993) 290; (c) P.E.M. Siegbahn, *J. Organomet. Chem.*, *478* (1994) 83.

[7] M.R.A. Blomberg, C.A.M. Karlsson and P.E.M. Siegbahn, *J. Phys. Chem.*, *97* (1993) 9341.

[8] M.R.A. Blomberg, P.E.M. Siegbahn and M. Svensson, *J. Am. Chem. Soc.*, *114* (1992) 6095.

[9] M.R.A. Blomberg, P.E.M. Siegbahn and M. Svensson, *J. Phys. Chem.*, *98* (1994) 2062.

[10] P.E.M. Siegbahn, M.R.A. Blomberg and M. Svensson, *J. Am. Chem. Soc.*, *115* (1993) 4191.

[11] P.E.M. Siegbahn and M.R.A. Blomberg, *Organometallics*, *13* (1994) 354.

[12] T. Sakakura, T. Sodeyama, K. Sasaki, K. Wada and M. Tanaka, *J. Am. Chem. Soc.*, *112* (1990) 7221.

[13] H. Kawamura-Kuribayashi, N. Koga and K. Morokuma, *J. Am. Chem. Soc.*, *114* (1992) 8687.

[14] L.A. Castonguay and A.K. Rappe', *J. Am. Chem. Soc.*, *114* (1992) 5832.

[15] (a) A.H. Janowicz and R.G. Bergman, *J. Am. Chem. Soc.*, *104* (1982) 352; (b) A.H. Janowicz and R.G. Bergman, *J. Am. Chem. Soc.*, *105* (1983) 3929.

[16] (a) J.K. Hoyano and W.A.G. Graham, *J. Am. Chem. Soc.*, *104* (1982) 3723; (b) J.K. Hoyano, A.D. McMaster and W.A.G. Graham, *J. Am. Chem. Soc.*, *105* (1983) 7190.

[17] W.D. Jones and F.J. Feher, *J. Am. Chem. Soc.*, *104* (1982) 4240.

[18] (a) M. Blomberg, U. Brandemark, L. Pettersson and P. Siegbahn, *Int. J. Quantum Chem.*, *23* (1983) 855; (b) M.R.A. Blomberg, U. Brandemark and P.E.M. Siegbahn, *J. Am. Chem. Soc.*, *105* (1983) 5557; (c) M.R.A. Blomberg, J. Schüle and P.E.M. Siegbahn, *J. Am. Chem. Soc.*, *111* (1989) 6156; (d) M.R.A. Blomberg, P.E.M. Siegbahn, U. Nagashima and J. Wennerberg, *J. Am. Chem. Soc.*, *113* (1991) 476; (e) M.R.A. Blomberg, P.E.M. Siegbahn and M. Svensson, *J. Phys. Chem.*, *95* (1991) 4313, (f) M.R.A. Blomberg, P.E.M. Siegbahn and M. Svensson, *New J. Chem.*, *15* (1991) 727. (g) M. Svensson, M.R.A. Blomberg and P.E.M. Siegbahn, *J. Am. Chem. Soc.*, *113* (1991) 7077.

[19] (a) J.J. Low and W.A. Goddard III, *J. Am. Chem. Soc.*, *106* (1984) 8321; (b) J.J. Low and W.A. Goddard III, *Organometallics*, *5* (1986) 609; (c) J.J. Low and W.A. Goddard III, *J. Am. Chem. Soc.*, *106* (1984) 6928; (d) J.J. Low and W.A. Goddard III, *J. Am. Chem. Soc.*, *108* (1986) 6115.

[20] B. Meunier, B. Chaudret (Eds.), *Perspectives in the Selective Activation of C–H and C–C Bonds in Saturated Hydrocarbons*, Scientific Affairs Division-NATO, Brussels, 1988.

[21] (a) C.W. Bauschlicher, Jr., S.R. Langhoff, H. Partridge and L.A. Barnes, *J. Chem. Phys.*, *91* (1989) 2399; (b) M. Rosi, C.W. Bauschlicher, Jr., S.R. Langhoff and H. Partridge, *J. Phys. Chem.*, *94* (1990) 8656.

[22] (a) E.A. Carter and W.A. Goddard III, *J. Phys. Chem.*, *92* (1988) 5679; (b) E.A. Carter and W.A. Goddard III, *J. Am. Chem. Soc.*, *108* (1986) 2180.

[23] M.R.A. Blomberg, P.E.M. Siegbahn and M. Svensson, *New J. Chem.*, *15* (1991) 727.

[24] P.E.M. Siegbahn, *Theor. Chim. Acta.*, *86* (1993) 219.

[25] M.W. Schmidt, K.K. Baldridge, J.A. Boatz, J.H. Jensen, S. Koseki, M.S. Gordon, K.A. Nguyen, T.L. Windus and S.T. Elbert, GAMESS (*General Atomic and Molecular Electronic Structure System*), *OCPE Bulletin*, *10* (1990) 52.

[26] P.E.M. Siegbahn and M. Svensson, *Chem. Phys. Lett.*, *216* (1993) 147.

[27] D.P. Chong and S.R. Langhoff, *J. Chem. Phys.*, *84* (1986) 5606.

[28] R.L. Martin, *J. Phys. Chem.*, *87* (1983) 750. See also R.D. Cowan and D.C. Griffin, *J. Opt. Soc. Am.*, *66* (1976) 1010.

[29] STOCKHOLM is a general-purpose quantum chemical set of programs written by P.E.M. Siegbahn, M.R.A. Blomberg, L.G.M. Pettersson, B.O. Roos and J. Almlöf.

[30] P.E.M. Siegbahn, M.R.A. Blomberg and M. Svensson, *Chem. Phys. Lett.*, *223* (1994) 35.

[31] B.G. Johnson, P.M.W. Gill and J.A. Pople, *J. Chem. Phys.*, *97* (1992) 7846.

[32] GRADSCF is a vectorized SCF first- and second-derivative code written by A. Komornicki and H. King.

[33] S.A. Mitchell, M.A. Blitz, P.E.M. Siegbahn and M. Svensson, *J. Chem. Phys.*, *100* (1994) 423.